# Appendices

# Appendix 1

Publication arising from this work:

Davidson, RA 2001, 'Determination of radiographic characteristics of tissue compensation filters using a Compton scatter technique', *Australian Physical & Engineering Sciences in Medicine*, vol. 24, no. 3, pp. 166-171.

**Determination of radiographic characteristics of tissue compensation filters using a Compton scatter technique.**

Tissue compensation filters (TCF) aid in plain film radiographic examinations by reducing the range of radiographic densities in the film. The composition and shape of the TCF assists in reducing radiographic density ranges that result from large anatomical density differences within the patient. A Compton scatter technique has been used to examine x-ray spectra from various TCF materials and thicknesses. Advantages and disadvantages of the Compton scatter technique in the examination of TCF under clinical conditions are discussed. Conclusions have been reached that will allow clinicians to optimise radiographic factors when performing radiographic examinations using TCF. In addition, conclusions have been drawn to determine the most appropriate clinical conditions for use of TCF and how dose to the patient will be affected.

## Introduction

Tissue compensation filters (TCF) are used in radiographic plain film examinations to selectively reduce resultant radiographic density ranges within the image (Butler *et al,* 1986; Gray, Hoffman & Peterson 1983; Petersen & Rohr, 1987). By locating the TCF within the x-ray beam in relation to the patient's anatomy, large radiographic densities differences due to anatomical density variations can be reduced. This is achieved through attenuation hence reducing the number of photon in the x-ray beam. The resultant range of radiographic density ranges is reduced which improves the perceived quality of the radiographic image. The major objective of the TCF is then to improve the diagnostic information within the radiograph. The confidence of clinician to make a correct diagnosis is then increased.

Tissue compensation filters are x-ray attenuating materials which are shaped for a specific anatomical area being examined. These filters differ in purpose from inherent and additional filtration within the x-ray beam. Inherent and additional filters reduce the number of low energy x-ray photons in the beam and hence reduces patient dose.

A few authors have examined tissue compensation filters. Butler *et al* (1986); Gray, Hoffman & Peterson (1983); Petersen & Rohr (1987) have examined selected aspects of the characteristics of specific tissue compensation filters. Butler *et al* (1986) and Gray *et al* (1983a) have only examined the use of tissue compensation filters in the examination of scoliosis and Petersen & Rohr (1987) for their use in lower extremity examinations. Radiation dose reduction and subjective assessment of image quality have been these authors' only assessment of tissue compensation filter characteristics. Dose reduction has also been examined by Gray, Stears & Frank (1983). Other author, Koedoorer & Venema (1986); Kohns, Gooch & Keller (1988); MacDonald-Jankowski & Lawinski (1992) and Regano & Sutton (1992) have looked at the value of additional filtration's role in patient dose reduction. Carrier & Beique (1992) and Sandborg *et al* (1994) have examined the spectral changes of the beam due to the use of additional filtration. These authors' focus was primarily dose related although contrast changes resulting from the use of additional filtration was also discussed.

The project undertaken here has attempted to further analyse tissue compensation filters other than those undertaken by the above authors.

## Research Objectives

The primary objective of the project is to determine the most appropriate clinical radiographic conditions for the use of the TCF.

The addition of attenuating material within a x-ray beam will increase the effective energy of that x-ray beam, due to the greater attenuation of low energy photons over higher energy photons within the polychromatic beam (Curry, 1990). This change in the effective energy or the x-ray beam's mean energy is also known as spectral shift. The further addition of amounts of attenuating material to the x-ray beam will further increase the spectral shift of the beam. By evaluation of the spectral changes that result from increasing thicknesses of TCF within the x-ray beam, conclusions about clinical characteristics may be drawn.

In this project commercially available TCF have been analysed under various clinical diagnostic radiographic conditions to determine the most appropriate energy level, that is the kVp setting, of the x-ray beam. The x-ray generator type for which the TCF is the most effective' has also been determined. Dose conclusion will also be drawn from the examination of the x-ray spectra.

## Research Methodology

The method of analysis has been to evaluate the changes in the x-ray beam's spectrum resulting from the placement of various thicknesses of the TCF in the x-ray beam. Attenuation changes for each x-ray photon energy range within the x-ray beam have been examined. From this examination, the effectiveness of the TCF has been related to the mean energy shift of the beam with increasing TCF thickness within the x-ray beam.

A Compton spectrometer (provided courtesy the Australian Radiation Laboratories, Melbourne) has been used for the x-ray spectral analysis. The Compton spectrometer (Matscheko, 1988) collects scattered Compton photons at approximately 90° from the direction of the primary beam (Figure 1). These photons are scattered by lucite, a low atomic number material, and are collected by a germanium (HPGe) detector (Canberra Nuclear, USA). The collected photons, comprising the Compton spectrum, were then analysed using a multi-channel analyser (MCA) (APTEC, USA). The Compton spectra were then converted to primary beam spectra.

Three different tissue compensation filters were used in this project, comprising lead-impregnated rubber (Octostop, Canada), lead acrylic (Nuclear Associates, USA), and aluminium composite (Grey Tech Services, Australia). The shape of the tissue compensation filters used was that of a wedge. Three different thicknesses of each tissue compensation filter were aligned in the primary beam prior to the beam's entry into the Compton spectrometer (Position A in Figure 1).

Further, three diagnostic x-ray units typical of those found in clinical radiology departments were selected. These were a single phase, 2 pulse, 100% ripple generator (Toshiba, Australia); a three phase, 12 pulse, approximately 6% ripple generator (Toshiba, Australia) and a single phase, medium frequency, approximately 3% ripple generator (Toshiba, Australia).

Maximum x-ray beam energies of typical clinical diagnostic radiographic examinations were chosen. The settings used were 60, 70, 80, 90 and 100 kVp.

X-ray spectra were collected from three thicknesses of each TCF using each generator type at each beam energy level. Additionally, spectra were obtained from each generator type at each beam energy level without any TCF within the beam.

Comparison of the spectra, for each combination, was then made visually and statistically. Conclusions based on these comparisons have been reached.

## Compton scatter technique

The main problem when using high energy photon detectors and MCAs to capture x-ray spectra is their limited countrate capabilities (Matscheko, 1988). Once this countrate limit is exceeded, a phenomena known as “pulse pile-up” results causing inaccuracies in the collected data. Several techniques can be used to overcome the problem of “pulse pile-up”. For this project, the Compton scatter technique was chosen.

The Compton spectrometer, which utilises Compton scatter technique, is illustrated in Figure 1. The prime objective of the Compton spectrometer is to maximise the probability that the photons detected are Compton photons that have been scattered at approximately 90° to the path of the primary photons. As shown in Figure 1, the primary beam is directed through an aperture (A) in the Compton spectrometer. The primary scatter chamber’s (B) role is to attenuate forward scatter of the primary beam from the aperture edges and reduce the likelihood of these photon reaching the scattering rod. In the next chamber, a low atomic number material rod is placed in the path of the primary beam. The role of the rod is to scatter the primary beam photons. The rod is constructed of low atomic number material which aids in the predominance of Compton scatter (Matscheko & Ribberfor, 1987). The scattering rod can be constructed at different diameters. The diameter of the rod will affect number of photons that are scattered hence the numbers of photons that reach the detector. The diameter will also affect the likelihood of the photon incurring secondary interactions on it passage out of the rod. Photons that have incurred secondary interactions that reach the detector will contribute to the reconstructed spectra and hence reduce the resolution of the final spectra. The chamber in which the rod is situated has a region (above E) for the exit of the scattered photons towards the detector. Alignment of the scattering rod with the exit region and with the detector aperture (G) can be viewed through aperture D. Secondary scatter chambers

(F) reduce the number of photons that have undergone secondary interactions or that are scattered from the exit region edges (above E) reaching the detector.

The Compton spectrometer has the advantage of ease of use and alignment of equipment under clinical conditions over other photon reduction techniques.

Matscheko (1988) states the main disadvantage with this method of x-ray spectral analysis is the decrease in energy resolution due to scattering geometry and Compton broadening. Matscheko (1988) further state that measurements of relative spectra are accurate to within 1%. Martin and Burns (1992) state that HPGe detectors are well suited for low energy ranges of 25 – 80 keV. The Compton spectrometer use in conjunction with an HPGe detector would therefore allow accurate spectral comparison and analysis.

Following collection of the Compton spectral data, an algorithm was utilised on a standard IBM PC based computer to reconstruct the primary beam spectra from the collected Compton photon data. There are 2 major requirements of the algorithm (Matscheko, 1988). The first is to determine the primary photon's energy that resulted in a Compton photon of detected energy and next, to determine the number of photons in the primary beam that resulted in the number of Compton photons detected.

The first requirement of the algorithm is met through using the well-known Compton equation.

Compton equation
$$h\nu_c = \frac{h\nu_0 . mc^2}{(mc^2 + h\nu_0(1-\cos\theta))} \qquad (1)$$

where $h\nu_c$ is energy of the scattered photon
$h\nu_0$ is energy of the primary photon
$mc^2$ is rest energy of the electron
$\theta$ is the angle of scatter

The Compton equation relates the energy of the primary photons, $h\nu_0$, to the energy of scattered photon, $h\nu_c$, through a scatter angle, $\theta$. The Compton spectrometer utilises $\theta$ at 90°.

The second requirement of the algorithm is to determine the number of photons, $N_{h\nu}(h\nu_0)$, in the primary beam at the energy $h\nu_0$. The number of detected Compton photons, $N_{h\nu}(h\nu_c)$, is a result of a combination of the number of primary photons, scatterer material type and volume of the scatterer "seen" by the detector. Scatter material and volume (diameter and length) will determine number of electrons, $N_e$, in scatterer and hence the probability that an interaction resulting in Compton scatter will occur (Matscheko & Ribberfor, 1987). As stated above, increasing the diameter of the scatter will also decrease the resolution of the reconstructed spectrum.

An assumption of the algorithm is the magnitude of the scattering cross sections for coherent and incoherent scattering at the examined energy levels. Where primary photon energy, $h\nu_0$, is greater than 35keV and the scattering angle, $\theta$, is 90°, the number of the coherently scatter photons reaching the detector is approximately zero.

Where $h\nu_0$ is less than 35keV and $\theta$ is 90°, the number of the coherently and incoherently scattered photons contribution at the detector is approximately equal (Matscheko, 1998). The contribution of coherently scattered photons reaching the detector increases as $h\nu_0$ decreases. Predominance of incoherently scattered photons reaching the detector is maintained through the use of low atomic number material (Matscheko & Ribberfor, 1987).

Figure 2 shows a comparison of the Compton spectrum, obtained using a 3% ripple generator and a generator setting of 100 kVp, and the resultant reconstructed spectrum. The Compton spectrum photon count has been scaled by a factor of 4.8 x $10^4$ for ease of comparison. The algorithms energy and photon number scaling is clearly represented.

## Limitations of the Compton Spectrometer

In this project the Compton scatter technique was used to overcome the problem of limited count-rates accepted by MCAs, that is the problem of pulse pile-up. (Matscheko, 1988) Under clinical radiographic conditions used during the project, the use of the Compton scatter technique led to an additional problem, that of noisy data.

Low photon counts at each energy range being detected for a given channel of the MCA, caused statistical variations between adjacent channels leading to the appearance of noisy data. Initially the MCA utilised 1024 channels with an energy range (channel width) of less than 0.1 keV per channel. To reduce the appearance of noise within the spectra, 256 channel where used in the MCA with a width per channel of approximately 0.37 keV. All spectra were collected using 256 channels in the MCA.

The appearance of noise within the spectra was reduced but not eliminated (see Figure 3). Visual comparison of spectra from differing generators, maximum beam energy (kVp) settings and tissue compensation filter thicknesses was still difficult with this level of noise within the data.

Several methods were further evaluated to further reduce the noise within the spectra. Increasing the statistical photon count, so the signal to noise ratio (SNR) would be increased, was the first method evaluated. The means of increasing the statistical photon count within an x-ray beam is to increase the combination of x-ray tube current (mA) and exposure time. The heat rating of the x-ray tube limits this combination in a single exposure. Increasing the number of exposures, allowing for x-ray tube cooling, will increase the statistical photon count collected by the detector. A comparison of spectra obtained using 20, 50, 75 and 100 exposures is shown in figure 4. Figure 4 clearly shows that resolution improves as the SNR of the spectra increases. Note, in Figure 4, the improvement of resolution of the Kα and Kβ spectral peaks from the Tungsten target as the number of exposures taken increases.

Using exposure numbers of this magnitude proved unacceptable due to the time taken to collect each spectra and heat load limits on the x-ray tube and generator. An exposure number of four and x-ray tube current of 400mA for a duration of 1 second

were used for the collection of each spectrum. These radiographic factors allowed a reasonable experimental time and were within x-ray tube ratings but still noise was present in the spectrum (see Fig. 3).

Methods to reduce noise within the spectra after collection of the spectral data, that of statistical filtering, were evaluated. After evaluating several signal filtering techniques, the filter chosen was that of a Savitzky-Golay filter as modified by Gander and von Matt (1995). The modified Savitzky-Golay filter algorithm allows user input to modify matrix size and vector length within the algorithm. Matrix size and vector length were chosen to optimise spectral appearance for noise reduction while maintaining kα and kβ spectral line sensitivity. Figure 5 shows a comparison of spectra that has been filtered using this modified Savitzky-Golay filter algorithm.

## Analysis

The conditions under which the spectral data was obtained were; without a tissue compensation filter within the primary x-ray beam; three thicknesses of each TCF; three different x-ray generators and five selected maximum beam energy (kVp). One hundred and fifty Compton spectra where collected, converted to primary beam spectra and filtered using the Savitzky-Golay filter. Each spectrum had a unique combination of TCF material type, TCF thickness (or no TCF), x-ray generator type and maximum beam energy (kVp). Each spectrum was obtained from four radiographic exposures each of an x-ray tube current of 400mA and 1 second exposure time.

Visual comparisons, although subjective by nature, provided an insight into the changes of the spectra resulting from the various conditions. Figures 6 and 7 give examples of such a visual comparison. Figure 6 is a comparison of unattenuated spectra and spectra of different TCF material. Figure 7 shows a comparison of unattenuated spectra and spectra of different thickness of lead impregnated rubber TCF material.

Statistical analysis of the effects of each additional thickness of the TCF was required to overcome the subjective nature of the visual comparison. The spectra, prior to being filtered using the Savitzky-Golay method, were used for the statistical analysis. The method used was that of calculating the weighted mean energy, $\bar{X}_W$ (keV), of each of the spectra. This weighted mean energy of the spectra could then be compared between spectra without TCF material present in the x-ray beam and for spectra with different TCF thicknesses placed within the x-ray beam. This comparison allows evaluation of the energy or spectral shift with changes in different filter thicknesses. Each TCF material attenuates the polychromatic x-ray beam differently. Manufacturers, depending upon the TCF material, will produce different thickness TCFs for the same radiographic task. To overcome differing thickness of TCF material between different manufacturers, the incremental spectral shift has been calculated. The incremental spectral shift is that change in the weighted mean energy that results from the addition of another thickness of TCF material to the x-ray beam.

Several terms need to be defined. These are:-

$$\text{Incremental Spectral Shift (keV)} = \frac{\overline{X}_{W1} - \overline{X}_{W0}}{\text{Fractional TCF Thickness}} \quad (2)$$

where:

$$\text{Fractional TCF Thickness} = \frac{\text{TCF Thickness 1 - TCF Thickness 0}}{\text{Maximum TCF Thickness}} \quad (3)$$

and

$\overline{X}_{W0}$ = weighted mean energy of the spectrum (keV)
$\overline{X}_{W1}$ = weighted mean energy of the spectrum with one additional filter thickness (keV)
TCF Thickness = measured filter thickness (mm)
Maximum TCF Thickness = that measured filter thickness of each filter as recommended by the manufacturer for the specific radiographic examination (mm)

The $\overline{X}_W$ and incremental spectral shift was also calculated for the upper, middle and lower thirds of each the spectra. Each spectrum was divided into thirds for the calculation of the $\overline{X}_W$ of that third of the spectrum. The upper and lower bounds of each third of the spectra where defined using the maximum value of the photon energy within that spectrum, that is at approximately the kVp setting of the generator. Incremental spectral shift for each third of the spectrum was calculated as per the method described above. The analysis of the incremental spectral shift within each of these thirds would allow conclusions to be drawn about the TCF's affect on spectral shape and patient dose that resulted from the use of each TCF.

The incremental spectral shift values were plotted for each maximum energy level (kVp), that is, at each generator setting of the spectra. This was undertaken for each different generator type. This has allowed the effects of the TCF material on the changes to the spectrum to be evaluated (see Figure 8). Figures 9, 10, & 11 show the effects of the TCF material for the upper, middle and lower thirds of the spectra. The incremental spectral shift data for each generator type (100%, 6% and 3% ripple) has been combined in Figures 8, 9, 10 and 11 for the purpose of displaying the data. Spectral shift data has also been plotted so changes that result from the generator type can be evaluated (see Figure 12).

## Results

Lead impregnated rubber (Pb R) TCF produced less incremental spectral shift than the lead acrylic (Pb A) TCF and the aluminium composite (Al) TCF across all three generator waveform. The composite plots for the three generator are shown in Figure 8. Only minor differences in incremental spectral shift occurred between the Pb A TCF and the Al TCF. The difference in incremental spectral shift between the Pb R TCF and the Pb A and Al TCF is seen to increase as the maximum energy of the beam (kVp) increased. From the plot, Figure 8, it can be seen that for the three TCF materials, maximum incremental spectral shift occurred for beams of kVp between 75 and 80 kVp.

On evaluation of the incremental spectral shift in the upper third of the spectra, TCF material had showed negligible difference on the amount of incremental spectral shift (Figure 9). It should be noted from this plot that in the upper third of the spectrum, incremental spectral shift increased at lower beam kVp and decreased at higher beam kVp.

In the middle third of the spectra, Pb A TCF and Al TCF's incremental spectral shift was similar (Figure 10). In this third of the spectra, Pb R TCF produced less incremental spectral shift than the Pb A TCF and the Al TCF. As the beams maximum energy (kVp) increased, the incremental spectral shift differences between Pb R TCF and the other two TCF increase.

Figure 11 shows the incremental spectral shift comparison for the three TCF materials in the lower third of the spectrum. The incremental spectral shift in this third of the spectra is negative, indicating the direction of the spectral shift between is to the left, for all TCF material. A spectral shift to the left results from $\bar{X}_{W0}$ being less than $\bar{X}_{W1}$. Beams of 60 to 70 kVp maximum energy show negligible differences in their incremental spectral shift. Above 70 kVp, the three TCF materials are causing a divergence of the amount of incremental spectral shift. Al C has the greatest incremental spectral shift with the incremental spectral shift of Pb R being the least. All three TCF materials provide the maximum incremental spectral shift when the beam's maximum energy is approximately 80 kVp.

Incremental spectral shift values, at each maximum beam energy, have been plotted in Figure 12. These values have been combined for all TCF material types for the purpose of displaying the plot. The incremental spectral shift values for the generators with 3% and 6% ripple waveforms were similar. At higher maximum energy beams, the incremental spectral shift values from the 100% ripple generator were increased compared to the results from the other two generator types.

## Conclusions

Several conclusions can be reached from the results. These conclusions will allow clinicians performing radiographic examinations to:-

- select an optimum kVp,
- have a knowledge of how the TCF will perform under various kVp settings,
- select the most appropriate TCF material for the examination,
- have a knowledge of how the TCF will perform when used with various generator types,
- have an indication of which TCF will additionally provide the greatest dose reduction benefit.

## Optimal Maximum Beam Energy (kVp)

Lead impregnated rubber TCF, lead acrylic TCF and aluminium composite TCF produced the greatest incremental spectral shift at maximum beam energies of approximately 75 – 80 kVp. This knowledge will allow clinicians to be able select a radiographic exposure so to achieve the greatest reduction of resultant radiographic

density ranges within the image. Radiographic examinations below this optimal kVp would not achieve the same density range reduction.

Tissue compensation filters

Lead acrylic TCF and aluminium composite TCF produced greater incremental spectral shift than the lead impregnated rubber TCF. Clinicians will be able to use this knowledge to select the most appropriate TCF material for a specific examination. Where patient anatomy density differences are large, the Pb A and Al TCF filters will achieve the greatest reduction in resultant image densities. . Where patient anatomy density differences are small, the Pb R TCF would be the TCF of choice for that radiographic examination.

Generator types

The results of the incremental spectral shift gained under various generator types are as would be expected from the theoretical knowledge of the waveforms from each generator type. The single phase, 2 pulse, 100% ripple generator has a much larger percentage of low energy photons than do generator types of three phase, 12 pulse, 6% ripple and single phase, medium frequency, 3% ripple (Curry, 1990). TCF have properties of added filtration in that they have increase attenuation at lower energy ranges. From this, it is expected that there would be increased incremental spectral shift resulting from the use of TCF in 100% ripple generators. The results discussed above confirm this.

Tissue compensation filters, when used with a 100% ripple generator, will have a greater effect on reduction of the resultant image densities. Clinicians can also use this knowledge when confronted with the choice of generator types for a radiographic examination. Their knowledge of how the TCF affect incremental spectral shift will aid in their acquisition of the radiographic image.

Dose reductions

The lower third of the spectra contains the lower energy photons of the x-ray beam which add to patient dose, especially skin dose. The aluminium composite TCF has the greatest effect on the incremental spectral shift in the lower third of the spectrum. From this, it can be concluded that the aluminium composite TCF will have the greatest effect on dose reduction to the patient. The dose reduction effects from PbA material where greater than when using PbIR material. Dose reduction effects will only be achieved when the TCF is placed in the beam prior to its entrance into the patient.

Additional Research

Validation of conclusions should be undertaken to confirm resultant image density changes from the use of the TCF. A range of maximum beam energies should be selected so to determine the image density changes under these conditions.

Dosimetry calculations, absorbed dose and entrance skin dose, should be performed under similar conditions to confirm the conclusions drawn from the data.

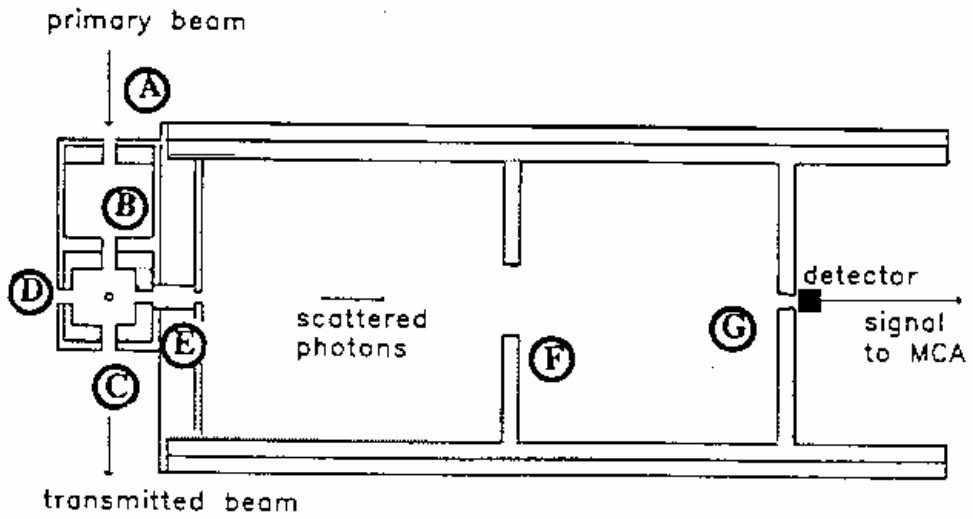


A. Entrance - Primary beam
B. Scatter Chamber - Primary beam photons
C. Transmitted beam
D. Line of Sight
E. Pb Shielding
F. Scatter Chamber - Scattered
G. Detector Aperture

Fig. 1. Compton Spectrometer (Matscheko, 1988)

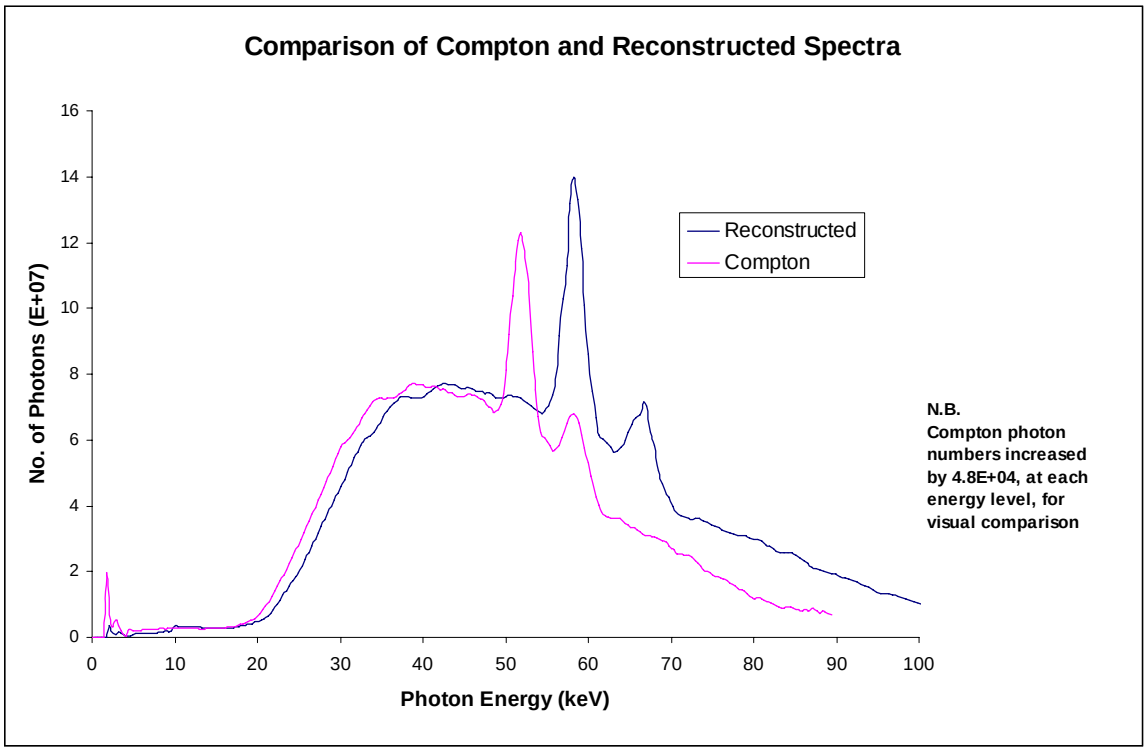


Fig. 2. Comparison of Compton and Reconstructed Spectra

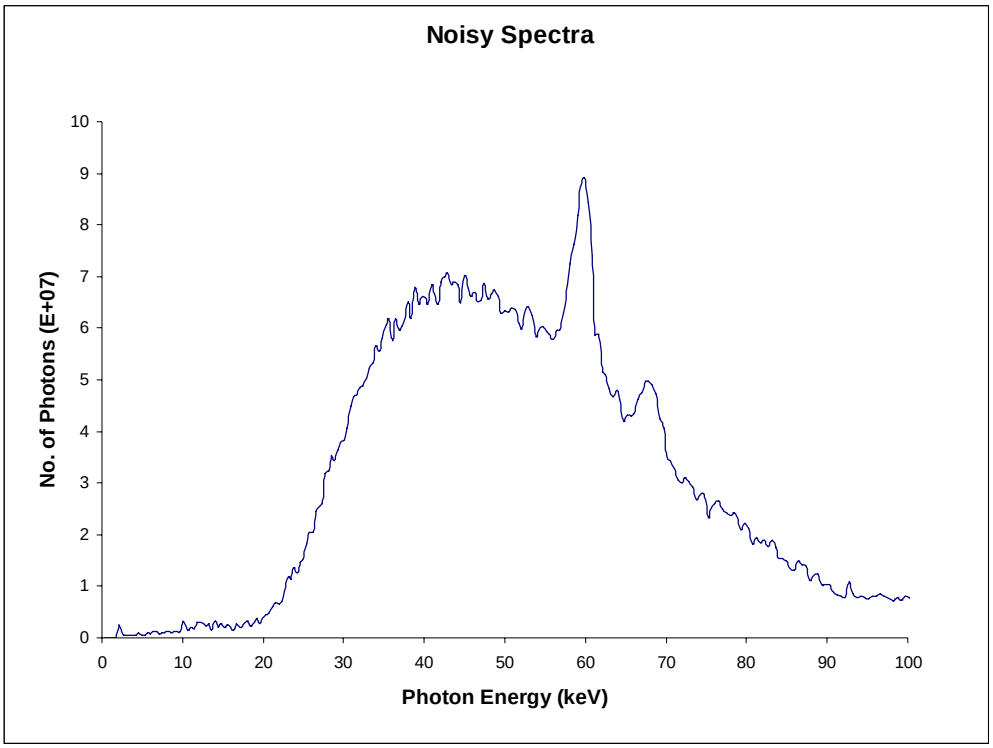


| | | | | |
|---|---|---|---|---|
| X-ray Unit Specifications | generator ripple | - 3% | tube voltage | - 90kVp |
| | target and angle | - W / 16 degrees | position in beam | - 0 degrees |
| | exposure | - 400mAs by 4 exp. | total filtration | - 2.2mm Al eq. |

Fig. 3. Noisy Spectrum due to Low Photon Counts

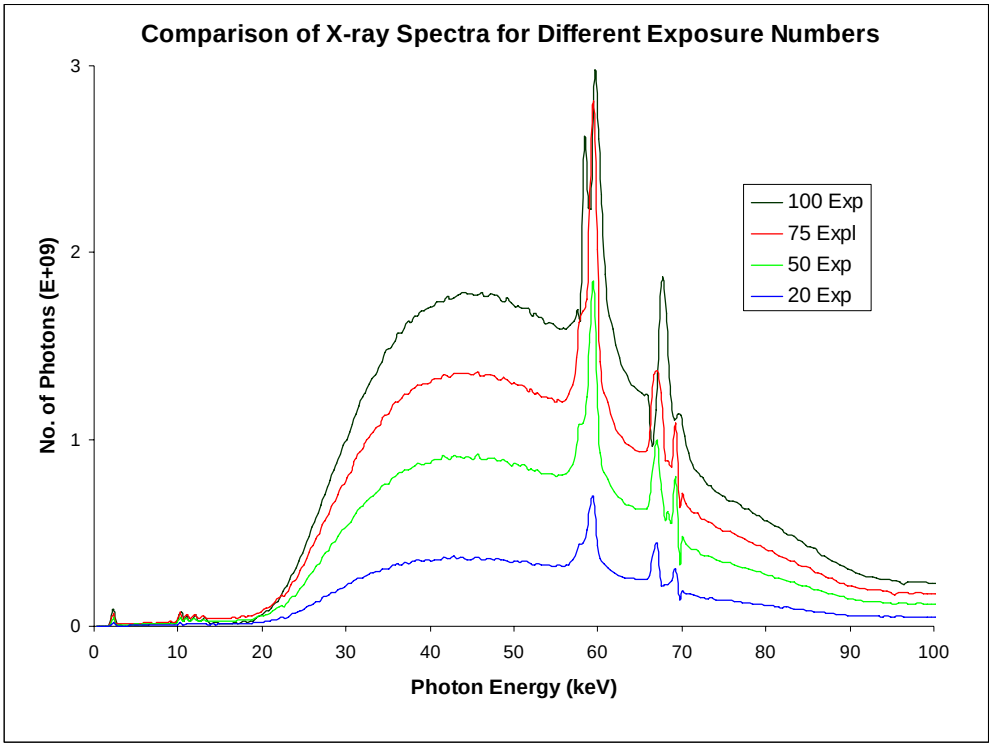


| | | | | |
|---|---|---|---|---|
| X-ray Unit Specifications | generator ripple | - 3% | tube voltage | - 90kVp |
| | target and angle | - W / 16 degrees | position in beam | - 0 degrees |
| | exposure | - 400mAs by n exp. | total filtration | - 2.2mm Al eq |

Fig. 4. Comparison of Exposure Numbers on SNR

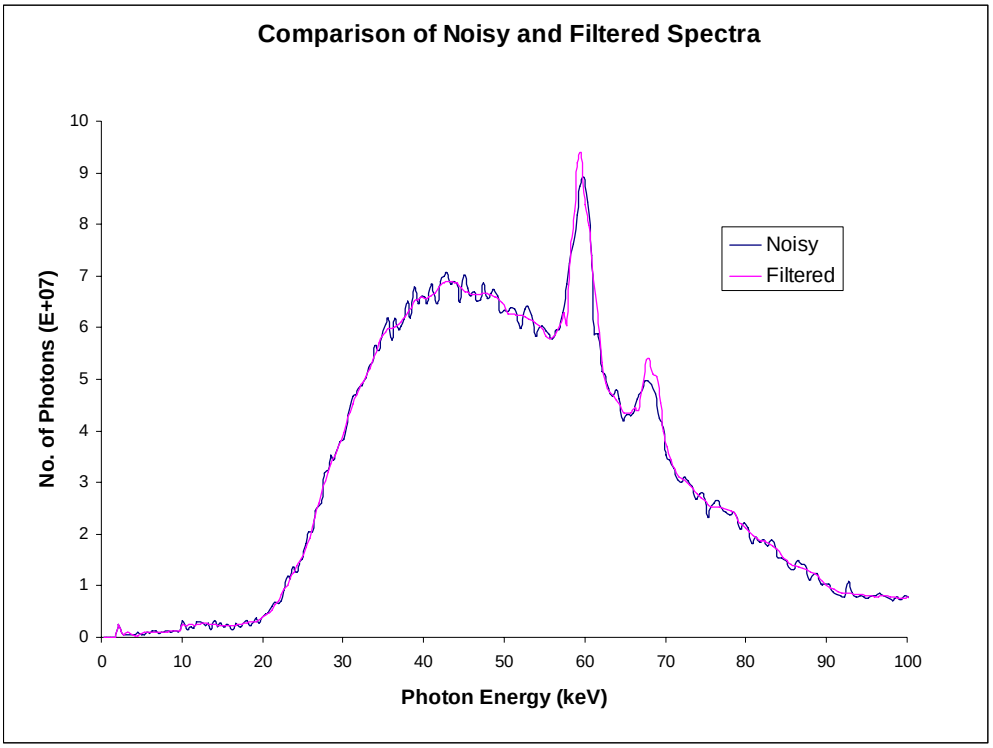


| | | | | |
|---|---|---|---|---|
| X-ray Unit Specifications | generator ripple | - 3% | tube voltage | - 90kVp |
| | target and angle | - W / 16 degrees | position in beam | - 0 degrees |
| | exposure | - 400mAs by 4 exp. | total filtration | - 2.2mm Al eq. |

Fig. 5. Noisy and Modified Savitzky-Golay Filtered Spectrum

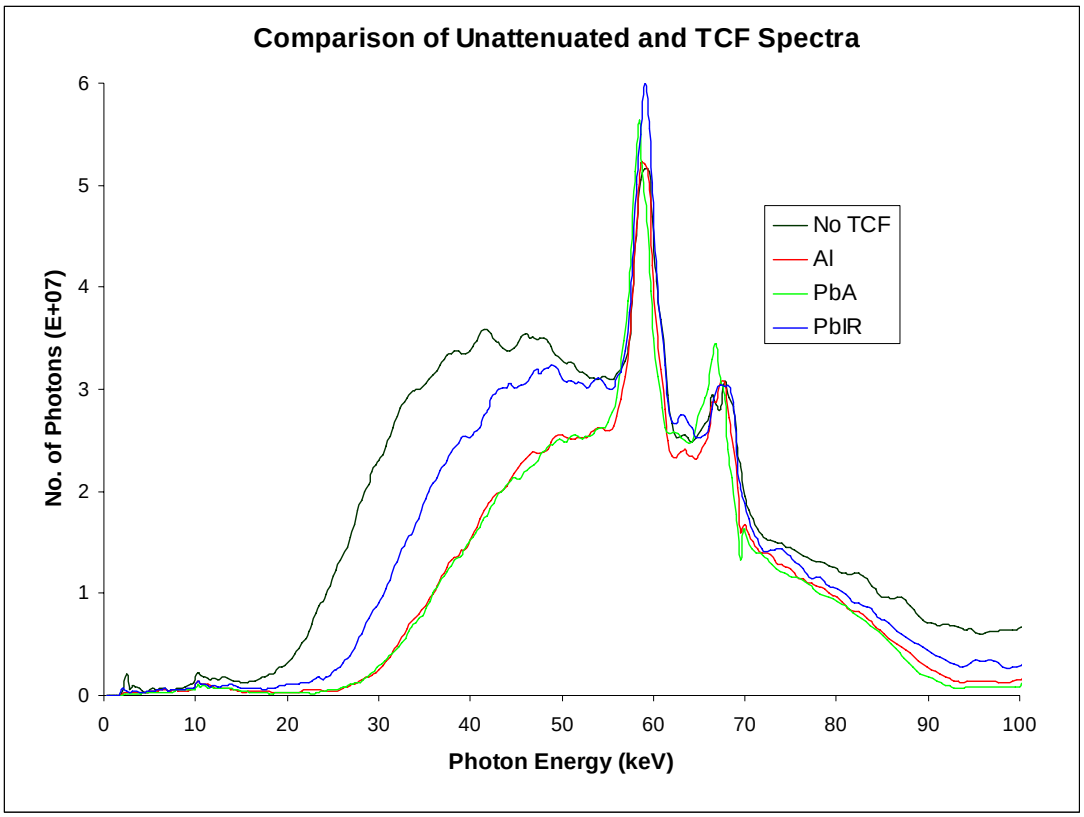


| X-ray Unit Specifications | | | | |
|---|---|---|---|---|
| | generator ripple | - 6% | tube voltage | - 90kVp |
| | target and angle | - W / 16 degrees | position in beam | - 0 degrees |
| | exposure | - 400mAs by 4 exp. | total filtration | - 2.2mm Al eq. |

Fig. 6. Visual Comparison of Unattenuated and Different TCF Spectra.

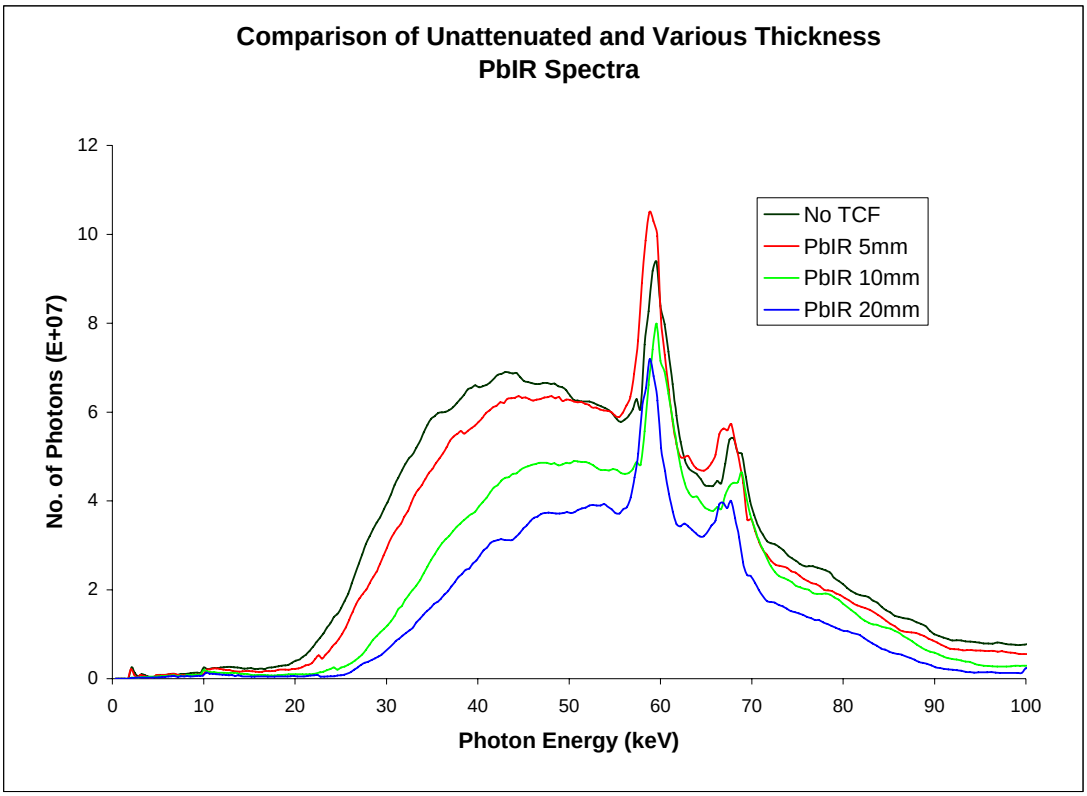


| X-ray Unit Specifications | | | | |
|---|---|---|---|---|
| | generator ripple | - 6% | tube voltage | - 90kVp |
| | target and angle | - W / 16 degrees | position in beam | - 0 degrees |
| | exposure | - 400mAs by 4 exp. | total filtration | - 2.2mm Al eq. |

Fig. 7. Visual Comparison of Unattenuated and Different PbIR Thickness TCF Spectra.

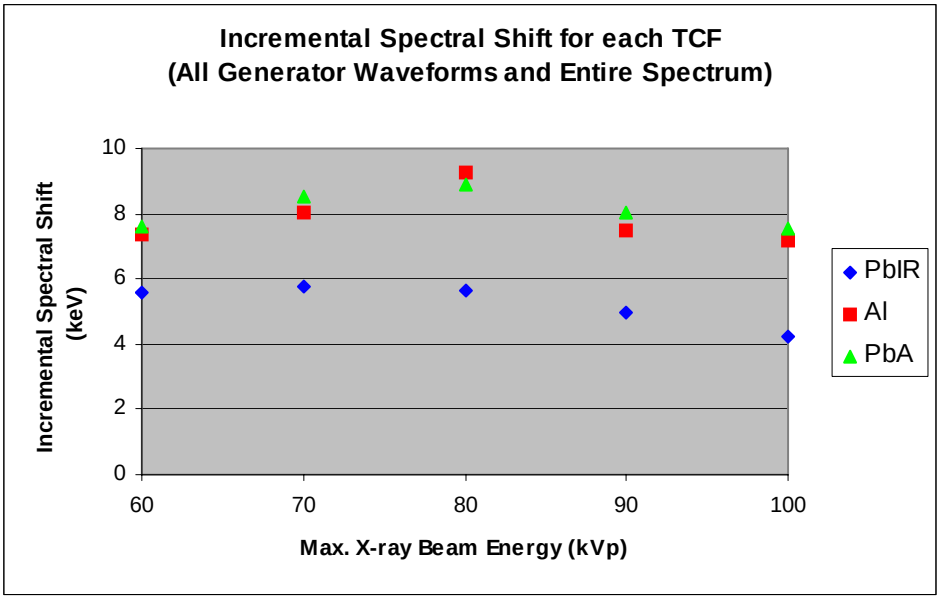


Fig. 8. Incremental spectral shift for each TCF (all generator waveforms and entire spectrum)

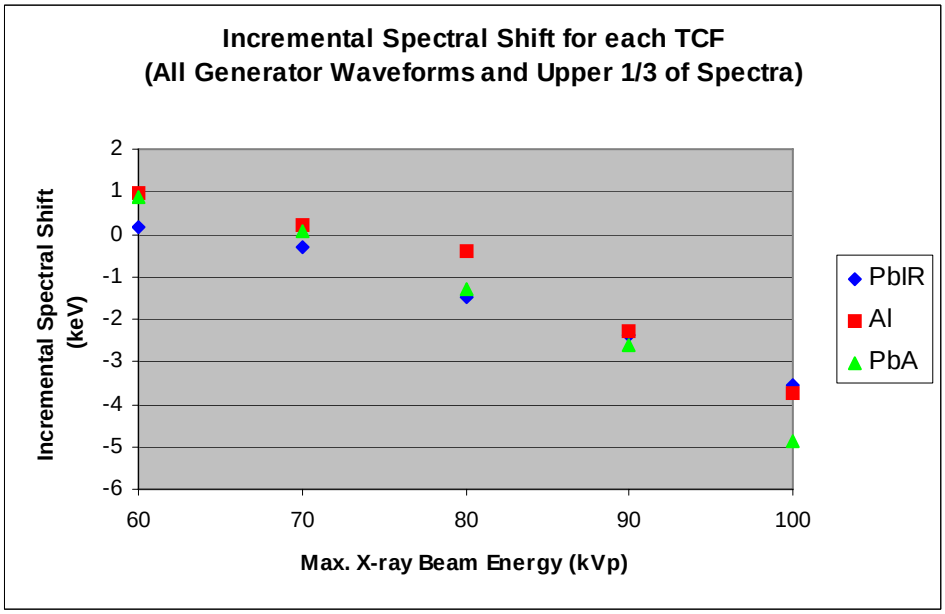


Fig. 9. Incremental spectral shift for each TCF (all generator waveforms and upper 1/3 of spectrum)

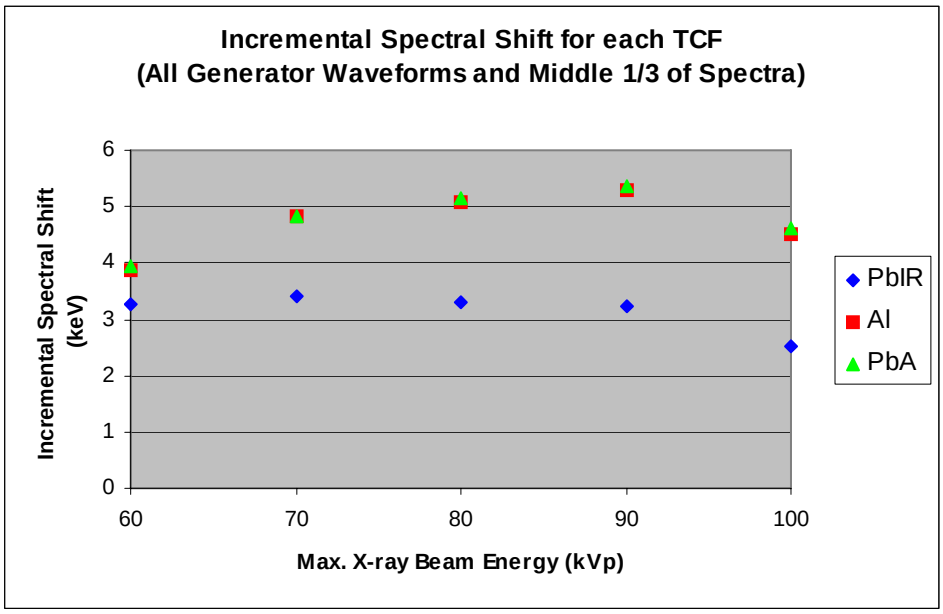


Fig. 10. Incremental spectral shift for each TCF (all generator waveforms and middle 1/3 of spectrum)

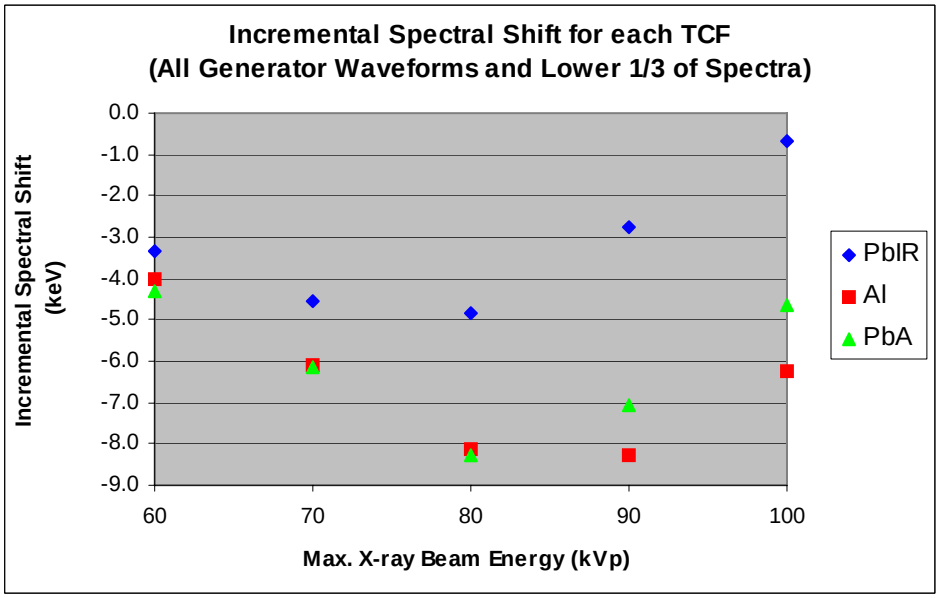


Fig. 11. Incremental spectral shift for each TCF (all generator waveforms and lower 1/3 of spectrum)

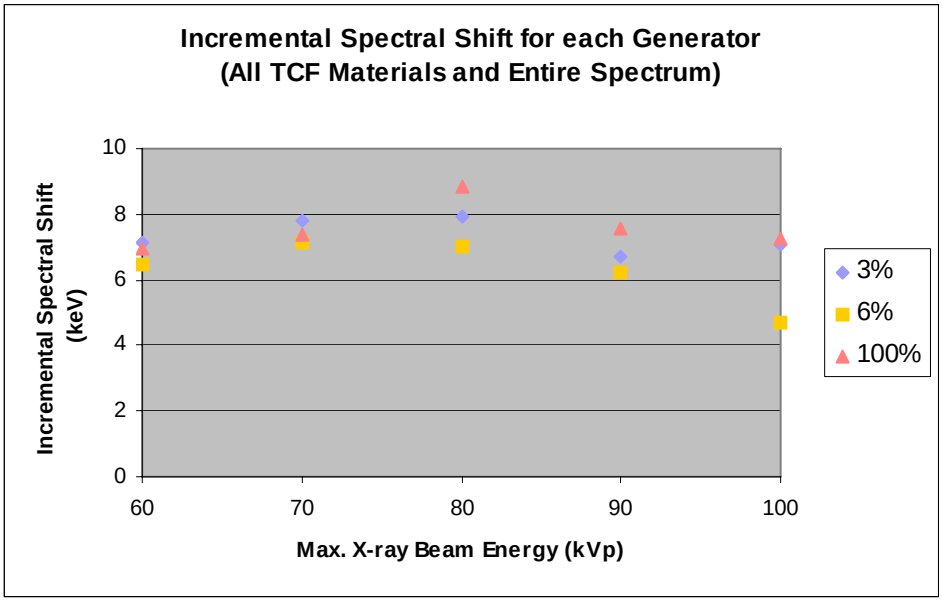


Fig. 12. Incremental spectral shift for each generator (all TCF material and entire spectrum)

**References**


Butler PF. Thomas AW. Thompson WE. Wollerton MA. and Rachlin JA. (1986) Simple methods to reduce patient exposure during scoliosis radiography, *Radiologic Technology*, 57(5) :411-417

Curry, T.S., Dowdey, J.E. and Murray, R.C., (1990) *Christensen's Physics of Diagnostic Radiology* (4th ed.), Lea and Febiger, Philadelphia

Gander W. and von Matt U. (1995) Smoothing Filters, in Gander W. and Hrebicek J., *Solving Problems in Scientific Computing Using Maple and Matlab*, 2nd Ed., Springer, Berlin

Gray JE. Hoffman AD. and Peterson HA. (1983) Reduction of radiation exposure during radiography for scoliosis, *Journal of Bone and Joint Surgery - American Volume*, 65A(1) :5-12

Gray JE. Stears JG. and Frank ED. (1983) Shaped, lead-loaded acrylic filters for patient exposure reduction and image-quality improvement, *Radiology*, 146 :825-828

Koedoorer K. and Venema HW. (1986) Filter material for dose reduction in screen-film radiography, *Physics in Medicine and Biology*, 31(6) :585-600

Kohns ML. Gooch AW. and Keller WS. (1988) Filters for radiation reduction: a comparison, *Radiology*, 167 :255-257

MacDonald-Jankowski DS. and Lawinski CP. (1992) The effect on thin K-edge filters on radiation dose in dental radiography, *British Journal of Radiology*, 65 :990-995

Martin LJ. and Burns PA. (1992) The HPGe as a defined-solid-angle detector for low energy photons, *Nuclear Instruments and Methods in Physics Research*, A312 :146-151

Matscheko G. (1988) A Compton spectrometer for measurement of primary photon energy spectra from clinical x-ray unit under working conditions, Unpublished PhD Dissertation, Linköping University Medical Dissertations, No. 280

Matscheko G. and Ribberfor R. (1987) A Compton scattering spectometer for determining x-ray photon energy spectra, *Physics in Medicine and Biology*, 32(5) :577-594

Petersen TD. and Rohr W. (1987) Improved assessment of lower extremity alignment using new roentgenographic techniques, *Clinical Orthopaedics & Related Research*, 219 :112-119

Regano LJ. and Sutton RA. (1992) Radiation dose reduction in diagnostic x-ray procedures, *Physics in Medicine and Biology*, 37(9) :1773-88

Sandborg M. Carlsson CA. and Carlsson GA. (1994) Shaping x-ray spectra with filters in x-ray diagnosis, *Medical & Biological Engineering & Computing,* 32(4) :384-90

Shrimpton PC. Jones DG. and Wall BF. (1988) The influence of tube filtration and potential on patient dose during x-ray examinations, *Physics in Medicine and Biology,* 33(10) :1205-1212

Villagran JE. Hobbs BB. and Taylor KW. (1978) Reduction of patient exposure by the use of heavy elements as radiation filters in diagnostic radiology, *Radiology,* 127 :249-254

# Appendix 2

Radiographic Contrast-Enhancement Mask Algorithms in Matlab® (MathWorks Inc., Natick, USA) m File Format

a. DICOM Read – opens and reads a DICOM image into MATLAB®
b. Wedge Radiographic Contrast-Enhancement Mask
c. Boomerang Radiographic Contrast-Enhancement Mask
d. Write Original Image – writes original image with new file name. Ensures patient details are erased
e. Write TCF Modified Image – writes modified image with new file name. Ensures patient details are erased

Legend

**%** words/characters that follow the "%" symbol until the end of the line are comments and do not form part of the algorithm.

**;** indicates the end of the code in that line. Line wrapping may have occurred following insertion into Microsoft Word® format

## Appendix 2a

DICOM Read

```
% Read a DICOM image and header information
% displays the image
clear all;

% directories of DICOM images
cd C:\Data\PhD\Surveys\Images\
% cd C:\data\PhD\DICOM\images\original\prospect;
% cd C:\Data\PhD\DICOM\Images\modified\not_filtered

[fname,fpath]=uigetfile('*.*');
cd(fpath);

I=double(dicomread(fname)); % read DICOM file to "I"

% NB Select only one of the following lines
I=4095*(I/max(max(I))); % set image to 12 bit and keep original greyscale
% I=4095-(4095*(I/max(max(I)))); % set image to 12 bit and invert greyscale

I=uint16(I); %convert to 16 bit image data

info=dicominfo(fname);
% low=info.WindowCenter(1)-(info.WindowWidth(1)/2);
% high=info.WindowCenter(1)+(info.WindowWidth(1)/2);
figure; imshow(I,[])

% writing a TIF file
%
% cd C:\data\PhD\DICOM\images\;
% imwrite(I,'test.tif','tiff','compression','none');
```

## Appendix 2b

Wedge Radiographic Contrast-Enhancement Mask

```
% Exponential or linear increase from top / bottom of image
% Flat section of filter at "thin" end of filter
% Reduces high (white) values at bottom of image

I=double(I); % from dicom_read.m
% I=100*ones(100,120); % select to obtain plots of filter
[rows, cols]=size(I);
disp(' ');
disp(' ');
disp('This filter will enhance the white or high value pixels');
disp(' ');
disp('It will initially be oriented to have the non-enhanced section');
disp('or "1" section at the top as viewed. Rotation can occur');
disp(' ');
disp('A gradient will occur between the top section and the bottom section');
disp('The strength of the enhancement of bottom section is achieved as an input');
disp(' ');
disp('To flip filter, rotate 180 degrees; Hit Return to leave as is');
rotd=input('Input: degree of rotation; - = cw; + = ccw; ');
if isempty(rotd)
   rotd = 0;
end
lyn=input('Input: length of non-enhanced section of filter as % eg 25; ');
if isempty(lyn)
   lyn = 0;
end
lyk=input('Input: length of enhanced section of filter as % eg 25; ');
if isempty(lyk)
   lyk = 0;
end
disp(' ');
gr=input('Input: value for type Gradient linear = l; curved = c; ','s');
if gr=='c'
   s=input('for curved: enter value between 2 & 3: lower value -> steeper slope; ');
end
disp(' ');
my=input('Input: strength of enhancement eg 2.5 (default = 2); ');
if isempty(my)
   my = 2;
end
my=my-1;
disp(' ');
```

```
if rotd == 90 | rotd == -90
   fwdth=rows;
   fhght=cols;
elseif rotd == 0
   fwdth=cols;
   fhght=rows;
else
   fwdth=round(cols * 1.5); % increase filter size so croping later
   fhght=round(rows * 1.5); % will not affect filter shape
end

% CREATING FILTER PROFILE
% sets a flat section of the filter
% flat section will at the "thinner" end, ie will = 1
flatk=fhght*lyk/100; % defines no. rows that are flat
flatn=fhght*lyn/100; % defines no. rows that are flat
x1=linspace(1,1,flatn-1); % creates flat section = 0
x3=linspace(1,1,flatk-1)*my; % creates flat section = 0
x2=linspace(1,my,fhght-(length(x1)+length(x3))); % creates even spaced values
between 0 & 1

if gr=='c'
   x=linspace(0,8,length(x2));
   x2=1/s*sqrt(2*pi)*exp(-x.^2/(2*s^2));
   minx2=min(x2);
   x2=x2-minx2;
   maxx2=max(x2);
   x2=x2/maxx2;
   x2=(x2*(1-my))+my;
end

x=[x1 x2 x3]; % joins 3 sections

% while size(x)<fhght % ensures size of filter = no. of rows
%     t=0;
%     x=[t x];
% end


% x=1+(x*my); % sets min value of filter to 1 and strength of filter

% Plots of filter when I=100*ones(100,100) selected
% figure; plot (x)

% grad=max(grad)-grad;
% grad=grad+my;

P=repmat(x,[fwdth 1]); % creates 2D filter
% rotates filter under user control
if rotd == 90 | rotd == -90
```

```
   if rotd == -90
      P=fliplr(P);
   end
   Imod=I.*P; %applies filter to original image

elseif rotd == 0
   P=P';      % orients filter to match image
   for i=1:cols
      for j=1:rows
        if P(j, i) == 0
           P(j, i)=1;
        end
      end
   end
   Imod=I.*P; %applies filter to original image

else
   P=P';      % orients filter to match image
   P=imrotate(P, rotd, 'crop');
   coldif=round((fwdth-rows)/2); % rematches filter to image size
   rowdif=round((fhght-rows)/2); %
   P=P(rowdif:rowdif+rows-1,coldif:coldif+cols-1); %& selects central section of
filter
   for i=1:cols
      for j=1:rows
        if P(j, i) == 0
           P(j, i)=1;
        end
      end
   end
   Imod=I.*P; %applies filter to original image
end

Imod=uint16(4095*(Imod/max(max(Imod)))); % set image to 12 bit
figure; imshow(Imod,[])
I=uint16(I);
```

## Appendix 2c

Boomerang Radiographic Contrast-Enhancement Mask

```
I=double(I); % from dicom_read.m
% I=100*ones(100,150); % select to obtain plots of filter
[rows, cols]=size(I);

side=input('Input: R or L shoulder? ','s');
switch side
case {'R','r','L','l'}
   ;
otherwise
   disp(' ')
   disp('Enter only R or L')
   return;
end

q=input('Input: Determine plan-view shape of filters / stretches filter to corner: 1 = diagonal line; 3 = nearly complete stretch; default factor = 2.5: ');
if isempty(q)
   q = 2.5;
end
my=input('Input: strength of filter - value > 1 required; default = 2; ');
if isempty(my)
   my = 2;
end
my=my-1; % 'my' reset later
s=input('Input: width of boomerang: 1 = narrow; 5 = broad; default = 2.5 ');
if isempty(s)
   s = 2.5;
end

% Creation of Filter
%
% Create Edge Shape of Filter
%
% uses q value from the user input
% shape edge of filter (for Rt Shoulder) - swap later
%
% determines shape of the edge of the filter
A=ones(rows+cols,2);
x=linspace(0,1,rows+cols);
y=linspace(1,0,rows+cols);
for i=1:rows+cols
   A(i,2)=max(min(round((x(i)^q)*cols),cols),1); % c value
end
```

```
for i=1:rows+cols
   A(i,1)=max(min(round((1-(y(i)^q))*rows),rows),1); % r value
end

% determines coordinants of the edge of the filter and
%    places values in filter at edge coordinants
S=sparse(A(:,1),A(:,2),ones(rows+cols,1),rows,cols);
filter=full(S);

% plot to check shape - not used for images
% figure; image(filter, 'CDataMapping','scaled'); axis image;

% Interpolation of Edge
%
%  modified from Hoff K, (1995) Bresenham's line algorithm,
%  http://www.cs.unc.edu/~hoff/projects/comp235/bresline/perform0.html
%  accessed 13/12/2001
filter(1,1)=1;
filter(rows,cols)=1;
% replaces filter edge values with '1'
for i=1:cols
   for j=1:rows
      if filter(j,i)>1
         filter(j,i)=1;
      end
   end
end

%  completes the filter's edge by filling in gaps in edge
%     in both vert & horiz directions
for i=1:cols
   for j=2:rows-1
      if filter(j-1,i)==1&filter(j,i)==0&filter(j+1,i)==1
         filter(j,i)=1;
      end
   end
end
for j=1:rows
   for i=2:cols-1
      if filter(j,i-1)==1&filter(j,i)==0&filter(j,i+1)==1
         filter(j,i)=1;
      end
   end
end
%  ensures continity of edge
for i=1:cols-1
   for j=1:rows-1
      if
filter(j,i)==1&filter(j+1,i)==0&filter(j,i+1)==0&filter(j+1,i)==0&filter(j+1,i+1)==0
         filter(j+1,i)=1;
```

```
      elseif filter(j,i)==1&filter(j+1,i)==0&filter(j,i+1)==0&filter(j+1,i+1)==1
        filter(j,i+1)=1;
      end
    end
end

% plot to check shape - not used for images
% figure; image(filter, 'CDataMapping','scaled'); axis image;

% filling a 2 column array with edge coordinates
[edge(:,1),edge(:,2)]=find(filter);


% Vertical Shape of Boomerang Filter
%
% create a normal distribution curve shape along a line
% applies curve along a line between bottom right corner and edge coordinates
%
% determines coordinates of line between edge and top right corner (filter
% oriented later) and populates matrix inside edge with values
%
% set parameters to determine shape
% "s" value (user input) sets range of distribution: lower numbers = narrow
%     distribution
% "s1" & "s2" values determine the portion of the normal distribution
%     curved used, with 0 being the centre of the curve
s1=-1;
s2=10;

for i=1:max(size(edge))
    a=[1 cols];
    b=edge(i,:);
    ly=abs(a(1,2)-b(1,2));% length, y dir, between points a & b
    lx=abs(a(1,1)-b(1,1));% length, x dir, between points a & b

    if ly>=lx
        T=ones(ly+1,2);
        x1=linspace(s1,s2,ly+1);
        y1=1/s*sqrt(2*pi)*exp(-x1.^2/(2*s^2));
        y1=fliplr(y1);
        T(1,:)=a;
        for j=1:ly
            T(j+1,2)=a(1,2)-j;
            T(j+1,1)=round(a(1,1)+(lx*j/ly));
        end
        for k=1:ly+1
            filter(T(k,1),T(k,2))=y1(k);
        end
    else
        T=ones(lx+1,2);
```

```
        T(1,1:2)=a;
        x1=linspace(s1,s2,lx+1);
        y1=1/s*sqrt(2*pi)*exp(-x1.^2/(2*s^2));
        y1=fliplr(y1);
        for j=1:lx
            T(j+1,2)=round(a(1,2)-(ly*j/lx));
            T(j+1,1)=a(1,1)+j;
        end
        for k=1:lx+1
            filter(T(k,1),T(k,2))=y1(k);
        end
    end
end

filter=flipud(filter); % orients filter up / down

% Normalise filter and allow user input for max strength of filter
maxval=max(max(filter));
filter=1+(my*(filter/maxval));

% allow user input to select R or L shoulder
switch side
case {'R','r'}
    ;
case {'L','l'}
    filter=fliplr(filter);
otherwise
    disp('Enter only R or L')
end

% figure; image(filter, 'CDataMapping','scaled'); axis image;
% figure, surf(filter); axis auto; axis ij;
% set(gcf,'Units','centimeters','Position',[10,10,20,10]);

Imod=filter.*I; % applies filter to image
Imod=4095*(Imod/max(max(Imod))); % set image to 12 bit
% mesh(Imod);
Imod=uint16(Imod);
figure; imshow(Imod,[])
I=uint16(I);
```

## Appendix 2d

Write Original Image

```
% Writing original DICOM Image

% NB. need to change ID and File Name

info.PatientID='Image_ID';
info.PatientsName.FamilyName=file_name;
info.PatientsName.GivenName='';

% Changes other fields - ensures these fields are blank
info.InstitutionName='';
info.InstitutionalDepartmentName='';
info.ReferringPhysiciansName='';
info.StationName='';
info.PatientsSex='';
info.PatientsBirthDate='';
info.PatientOrientation='';

% Changes Series ID for eFilm viewing
SeriesUID=info.SeriesInstanceUID;
len=size(SeriesUID);
len=len(:,2)-4;
SeriesUID_nos=double(int16(10000*rand));
SeriesUID=strcat(SeriesUID(1:len),int2str(SeriesUID_nos));

info.SeriesInstanceUID=SeriesUID;

% Select Directory and Write DICOM Image
cd C:\Data\PhD\DICOM\Images\test\shoulder
% cd C:\Data\PhD\Surveys\Images\D
status=dicomwrite(I,'file_name.dcm',info);
```

## Appendix 2e

Write TCF Modified Image

```
% Writing modified DICOM Image

% NB. need to change ID and File Name

info.PatientID='Image_ID';
info.PatientsName.FamilyName='file_name ';
info.PatientsName.GivenName='';

% Changes other fields - ensures these fields are blank
info.InstitutionName='';
info.InstitutionalDepartmentName='';
info.ReferringPhysiciansName='';
info.StationName='';
info.PatientsSex='';
info.PatientsBirthDate='';
info.PatientOrientation='';

% Changes Series ID for eFilm viewing
SeriesUID=info.SeriesInstanceUID;
len=size(SeriesUID);
len=len(:,2)-4;
SeriesUID_nos=double(int16(10000*rand));
SeriesUID=strcat(SeriesUID(1:len),int2str(SeriesUID_nos));

info.SeriesInstanceUID=SeriesUID;

% Select Directory and Write DICOM Image
cd C:\Data\PhD\Surveys\Images\temp
status2=dicomwrite(Imod,'file_name.dcm',info);
```

# Appendix 3

Participant Information Sheet

Note: The participant information sheet was written and sent to potential survey participants prior to transfer of candidature from Curtin University of Technology to The University of Sydney. The previous terminology of *Tissue Compensation Filters / Algorithms* was replaced with *Radiographic Contrast-Enhancement Masks / Algorithms*.

# Participant Information Sheet

Research Project: *Tissue Compensation Algorithms in Digital Radiography*

A Doctoral Research Project being undertaken through
Curtin University of Technology

Principal Investigator: Robert Davidson
Ph 02 69332503 (work)
Email: *rdavidson@csu.edu.au*
Department of Medical Imaging
Curtin University of Technology
PO Box U1987
Perth WA 6845

---

Thank you for agreeing to participate in this research project. It is expected that you will need approximately 40 minutes of your time to complete the review of the images and complete your responses. Please feel free to pass the CD ROM etc on to other interested radiographers or radiologists.

The purpose of the research project is to develop and evaluate tissue compensation filter algorithms for computed radiography (CR) images. The algorithms modify areas with in the image in order to improve overall displayed contrast and improved viewing of the anatomy in the image.

The package you have been provided includes:

- CD ROM
- blank 3½" floppy disk
- Participant Information Sheet and Participant Consent Form
- reply-paid envelop

The CD ROM contains 8 sets of CR images, each from a different anatomical region. A set of images will each contain an image that has been modified by the developed algorithm and the original, unmodified image. You will be asked to evaluate, through a questionnaire, which, in your opinion, is the preferred image. On the CD ROM will be a program, e*Film*, which will enable you to view the images. *eFilm* will also allow you to alter the viewing brightness & contrast of the images and alter the magnification of the images. Instructions are enclosed for the use of the program

The questionnaire has 2 sections. The first seeks some demographic data such as your profession and years of experience. Your identity will not be asked. The main section is seeking your opinion on a comparison between the 2 images. An example of a question is "Which image shows the best range of optical densities?" You will be asked to indicate your preferred image and then provide, on a scale from 1 to 5, the increase in improvement of your preferred image. Several other questions on each image will be asked.

You will need access to a personal computer running Windows® 95 or later. You may need to modify the monitor's settings to best visualise the images. Instructions for this are provided.

Please complete the Participant Consent Form and send it back to in the reply-paid envelop.

There are 3 options for completing the questionnaire. The first and preferred method is to complete it using a Microsoft™ Excel spreadsheet. The file, *Questionnaire Form.xls*, can be found on the CD ROM. Here you simply click on the appropriate response. If you do not have Excel, the alternative is complete the questionnaire using MS Word. The file, *Questionnaire Form.doc,* can be found on the CD ROM. With either method, the completed forms can be saved and emailed back to me or saved on the floppy disk provided and posted.
The 3rd option is to print the questionnaire form *(Questionnaire Form.doc* ),indicate you response on the form and post this back.

# Instructions

## Set-up of your personal computer.

On starting your computer and opening Windows®, right mouse click on the Desktop. A window will open. Scroll to and click on the "*Properties*" item in the menu. From the top menu tab, select "*Settings*". Ensure "Screen resolution" and "Color quality" are set on their highest value. Once you are using the program "*eFilm*" and viewing the images, you may need to experiment with the "Color quality" setting by altering the settings to ensure the optimal viewing of grey-scale images.

## Required files

All required files; the images and viewer; the Microsoft™ Excel and Microsoft™ Word response sheets and other documents are all on the CD ROM provided.
The CD ROM includes:

- *eFilm* viewer and associated files
- 8 sets of images of various anatomy
- *Questionnaire Form.xls* the questionnaire in Excel format
- *Questionnaire Form.doc* the questionnaire in Word format
- copies of the Consent Form and this Form in Word format

## Starting to view images

Insert the CD ROM into the CD ROM drive and shut the draw. The program *eFilm* should auto-start. If this does not occur, select *My Computer* from the Desktop. Select the CD ROM drive. Double click on the file *StartDICOM.bat* to start the viewer.

If this fails, you will need to run a program to install some files on your computer. Using *My Computer* go to the CD ROM drive and the *DICOM* directory. Double click the *DAO.exe* and allow this to run. Restart the *eFilm* viewer reinserting the CD

ROM in the drive. If after running this, *eFilm* still does not work run the *DAO.exe* from the *DAO* directory. (Different versions of DAO are for different operating systems)

For best viewing, ensure the viewer occupies the entire computer screen. If the viewer does not occupy the entire screen, select the middle button in the top right-hand corner of the viewer window. Positioning yourself and the monitor is important in optimising viewing conditions. Ensure you are directly in front the screen and not more that 1 metre from the monitor. The room should also be relatively dim with no direct light striking the monitor.

Opening Images

On opening *eFilm*, a list of image sets will be shown. Highlight an image set and select the *View* button. Two (2) images will open in the viewer. One image will be the original unmodified image and the other will have had a tissue compensation filter applied to it. There is no identifying data as to which image is which.

Each image has an ID and a name. The name will differ for both images in that set. The name is in the top row of information on the top right of each image and is information on the anatomical region and some numbers, for example "shoulder-A1-1" or "shoulder-A1-2". Please use the LAST number in the name to indicate your preferred image in the questionnaire, for example use "2" if you prefer the image "shoulder-A1-2". The image set ID is the 2nd row of information, eg, from the above example, the ID will be "A1". This ID information MUST be included on your answer / response sheet. Different CD ROMs have differing data sets. I need this information so I can assess your responses for that image set.

Changing Brightness and Contrast

Using the right mouse button, you can alter contrast and brightness (window width and level) of the image that the mouse cursor is over (note the brightness icon, a half sun, is already selected). Click and hold the right mouse button. Moving the cursor up and down will alter brightness and moving it sideways will alter contrast. Release the mouse button and the brightness and contrast will stay at that level. Move the mouse cursor over the other image and you will be able to alter the contrast and brightness of that image.

Magnify an Image

To magnify an image, select the magnifying glass icon on the top toolbar. Move the cursor over the desired image and click and hold the right mouse button to alter magnification. Select the arrowed cross from the toolbar and the left mouse button to move / scroll the image.

Close the Image and Open Another Image

To open another image select the cross (2nd from left) on the toolbar. This will close the image set and allow you to repeat the opening process described above.

**Questionnaire**

While viewing the image set, answer the questions in the appropriate section in the questionnaire.

Excel

Open MS Excel. The Excel questionnaire uses macros to assist in recording your responses. You may need to adjust your security level to enable the macros to run. Go to the *Tools* menu and select *Macro* and then *Security*. Select *Medium* or *Low*. If your security setting was *High* prior to do this, ensure you re-select *High* when you have finished and saved the questionnaire.

To open the Questionnaire, go to the *File* menu and select *Open*. Find the CD ROM drive and select *Questionnaire Form.xls*.

At the top of the form you will find some demographic data. Please complete this. Swap back to *eFilm* and the images you are evaluating. Answer the questions for each image set. When you have finished, insert the floppy disk into the floppy drive and from the *File* menu, select *Save As*. Find the Floppy Drive and select OK. The questionnaire will be saved on the Floppy Disk. You can post the floppy in the reply-paid envelop or email the file to me at *rdavidson@csu.edu.au*.

Word

Open MS Word. Do not close *eFilm*. To open the Questionnaire, go to the *File* menu and select *Open*. Find the CD ROM drive and select *Questionnaire Form.doc*. Complete the questionnaire as per the paragraph above, save on the file on the Floppy Disk and post the floppy in the reply-paid envelop or email the file to me.

Printed Questionnaire Form

If you are unable to complete either of the above electronic forms, please use this form and post the form back.

Again, thank you for your time and effort in assisting with this project. Please complete the Consent Form and post that back with the disk or response sheet (if you have not emailed it). Please contact me if you are having difficulties or need anything further.

Rob Davidson

# Appendix 4

Participant Consent Form

Note: The participant consent form was written and sent to potential survey participants prior to transfer of candidature from Curtin University of Technology to The University of Sydney. The previous terminology of *Tissue Compensation Filters / Algorithms* was replaced with *Radiographic Contrast-Enhancement Masks / Algorithms*.

# Participant Consent Form

Research Project: *Tissue Compensation Algorithms in Digital Radiography*

A Doctoral Research Project being undertaken through
Curtin University of Technology

Principal Investigator: Robert Davidson
Ph 02 69332503 (work)
Email: *rdavidson@csu.edu.au*
Department of Medical Imaging
Curtin University of Technology
PO Box U1987
Perth WA 6845

---

I, …….. consent to my participation in the research project titled, *Tissue Compensation Algorithms in Digital Radiography*.

I understand that I am free to withdraw my participation at anytime.

The purpose of the research has been explained to me and I have read and understood the information sheet given to me.

I permit the investigator to use my responses from the questionnaire as part of this project.

I understand that any information or personal details gathered in the course of this research about me are confidential and that neither my name nor any other identifying information will be used or published without my written permission.

Curtin University of Technology's Human Research Ethics Committee has approved this study. I understand that if I have any concerns or complaints about this research I can contact:

The Secretary
Human Research Ethics Committee
C/- Office of Research and Development
Curtin University of Technology
PO Box U1987
Perth WA 6845

Signed by: ……..

Date: ……..

## Appendix 5

Participant Questionnaire Form – Microsoft Word® Format

Note: The participant questionnaire form was written and sent to potential survey participants prior to transfer of candidature from Curtin University of Technology to The University of Sydney. The previous terminology of *Tissue Compensation Filters / Algorithms* was replaced with *Radiographic Contrast-Enhancement Masks / Algorithms*.

# *Participant Questionnaire Form*

Research Project: *Tissue Compensation Algorithms in Digital Radiography*
A Doctoral Research Project being undertaken through
Curtin University of Technology

Principal Investigator: Robert Davidson
Department of Medical Imaging
Curtin University of Technology
PO Box U1987
Perth WA 6845

Ph 02 69332503 (work)
Email: rdavidson@csu.edu.au

Please indicate your response by placing a cross in the underlined area.

Occupation

Radiographer _____ Radiologist _____ Other _____

if Other, please indicate _____

Experience

< 5 years ___ 5 – 10 years ___ 10 – 15 years ___ > 15 years ___

---

Response information

| Please enter the image ID in the box: eg. for shoulder: A1 ID's are found on the 2nd row of the image details |
|---|

| **Image Number Response** | **Scale Response Amount** when comparing images |
|---|---|
| Use the number in the "patient name" area. This is located in the top right hand corner of the image on the top row and is either “1” or “2” NB. The no. 1 image is not necessarily the left hand image | 1 very small; 2 small; 3 moderate; 4 large; 5 very large |

**Image Set Responses: Shoulder** Shoulder ID _____

A Which image shows the best range of optical densities? 1. ____ 2. ____

Please indicate the level of increase in improvement in range of optical densities. (using above scale) 1. ____ 2. ____ 3. ____ 4. ____ 5. ____

B In which image is all anatomy easiest to visualise? 1. ____ 2. ____

Please indicate the level of increase in improvement in ease of visualisation. (using above scale) 1. ____ 2. ____ 3. ____ 4. ____ 5. ____

C Which images allows for simplest contrast and density manipulation for optimal visualisation of all anatomy? 1. ____ 2. ____

Please indicate the level of increase in improvement in ease of optimisation. (using above scale) 1. ____ 2. ____ 3. ____ 4. ____ 5. ____

D Which of the images has the highest image quality? 1. ____ 2. ____

---

**Image Set Responses: C Spine** C Spine ID _____

A Which image shows the best range of optical densities? 1. ____ 2. ____

Please indicate the level of increase in improvement in range of optical densities. (using above scale) 1. ____ 2. ____ 3. ____ 4. ____ 5. ____

B In which image is all anatomy easiest to visualise? 1. ____ 2. ____

Please indicate the level of increase in improvement in ease of visualisation. (using above scale) 1. ____ 2. ____ 3. ____ 4. ____ 5. ____

C Which images allows for simplest contrast and density manipulation for optimal visualisation of all anatomy? 1. ____ 2. ____

Please indicate the level of increase in improvement in ease of optimisation. (using above scale) 1. ____ 2. ____ 3. ____ 4. ____ 5. ____

D Which of the images has the highest image quality? 1. ____ 2. ____

**Image Set Responses: T Spine** T Spine ID _____

A Which image shows the best range of optical densities? 1. ____ 2. ____

Please indicate the level of increase in improvement in range of optical densities. (using above scale) 1. ____ 2. ____ 3. ____ 4. ____ 5. ____

B In which image is all anatomy easiest to visualise? 1. ____ 2. ____

Please indicate the level of increase in improvement in ease of visualisation. (using above scale) 1. ____ 2. ____ 3. ____ 4. ____ 5. ____

C Which images allows for simplest contrast and density manipulation for optimal visualisation of all anatomy? 1. ____ 2. ____

Please indicate the level of increase in improvement in ease of optimisation. (using above scale) 1. ____ 2. ____ 3. ____ 4. ____ 5. ____

D Which of the images has the highest image quality? 1. ____ 2. ____

---

**Image Set Responses: T / L Spine** T / L Spine ID _____

A Which image shows the best range of optical densities? 1. ____ 2. ____

Please indicate the level of increase in improvement in range of optical densities. (using above scale) 1. ____ 2. ____ 3. ____ 4. ____ 5. ____

B In which image is all anatomy easiest to visualise? 1. ____ 2. ____

Please indicate the level of increase in improvement in ease of visualisation. (using above scale) 1. ____ 2. ____ 3. ____ 4. ____ 5. ____

C Which images allows for simplest contrast and density manipulation for optimal visualisation of all anatomy? 1. ____ 2. ____

Please indicate the level of increase in improvement in ease of optimisation. (using above scale) 1. ____ 2. ____ 3. ____ 4. ____ 5. ____

D Which of the images has the highest image quality? 1. ____ 2. ____

**Image Set Responses: Abdomen** Abdomen ID _____

A Which image shows the best range of optical densities? 1. ____ 2. ____

Please indicate the level of increase in improvement in range of optical densities. (using above scale) 1. ____ 2. ____ 3. ____ 4. ____ 5. ____

B In which image is all anatomy easiest to visualise? 1. ____ 2. ____

Please indicate the level of increase in improvement in ease of visualisation. (using above scale) 1. ____ 2. ____ 3. ____ 4. ____ 5. ____

C Which images allows for simplest contrast and density manipulation for optimal visualisation of all anatomy? 1. ____ 2. ____

Please indicate the level of increase in improvement in ease of optimisation. (using above scale) 1. ____ 2. ____ 3. ____ 4. ____ 5. ____

D Which of the images has the highest image quality? 1. ____ 2. ____

---

**Image Set Responses: Facial Bones** Facial Bones ID _____

A Which image shows the best range of optical densities? 1. ____ 2. ____

Please indicate the level of increase in improvement in range of optical densities. (using above scale) 1. ____ 2. ____ 3. ____ 4. ____ 5. ____

B In which image is all anatomy easiest to visualise? 1. ____ 2. ____

Please indicate the level of increase in improvement in ease of visualisation. (using above scale) 1. ____ 2. ____ 3. ____ 4. ____ 5. ____

C Which images allows for simplest contrast and density manipulation for optimal visualisation of all anatomy? 1. ____ 2. ____

Please indicate the level of increase in improvement in ease of optimisation. (using above scale) 1. ____ 2. ____ 3. ____ 4. ____ 5. ____

D Which of the images has the highest image quality? 1. ____ 2. ____

**Image Set Responses: Feet** Feet ID _____

A Which image shows the best range of optical densities? 1. ____ 2. ____

Please indicate the level of increase in improvement in range of optical densities. (using above scale) 1. ____ 2. ____ 3. ____ 4. ____ 5. ____

B In which image is all anatomy easiest to visualise? 1. ____ 2. ____

Please indicate the level of increase in improvement in ease of visualisation. (using above scale) 1. ____ 2. ____ 3. ____ 4. ____ 5. ____

C Which images allows for simplest contrast and density manipulation for optimal visualisation of all anatomy? 1. ____ 2. ____

Please indicate the level of increase in improvement in ease of optimisation. (using above scale) 1. ____ 2. ____ 3. ____ 4. ____ 5. ____

D Which of the images has the highest image quality? 1. ____ 2. ____

---

**Image Set Responses: Other Ext.** Other Ext ID _____

A Which image shows the best range of optical densities? 1. ____ 2. ____

Please indicate the level of increase in improvement in range of optical densities. (using above scale) 1. ____ 2. ____ 3. ____ 4. ____ 5. ____

B In which image is all anatomy easiest to visualise? 1. ____ 2. ____

Please indicate the level of increase in improvement in ease of visualisation. (using above scale) 1. ____ 2. ____ 3. ____ 4. ____ 5. ____

C Which images allows for simplest contrast and density manipulation for optimal visualisation of all anatomy? 1. ____ 2. ____

Please indicate the level of increase in improvement in ease of optimisation. (using above scale) 1. ____ 2. ____ 3. ____ 4. ____ 5. ____

D Which of the images has the highest image quality? 1. ____ 2. ____